

Table 1. Mutations in the GSK3 β phosphorylation consensus motif of the *Catnn**b* gene in colon tumors**

Mutated codon	Base change	Amino acid substitution†	No. mutations detected
32	GAT → AAT	Asp → Asn	8
33	TCT → TTT	Ser → Phe	4
34	GGA → GAA	Gly → Glu	8
37	TCT → TTT	Ser → Phe	2
41	ACC → ATC	Thr → Ile	4
44	CCT → CTT	Pro → Leu	1
45	TCC → TTC	Ser → Phe	2
Total			29

†Serine residues in codons 33, 37, and 45 and the threonine residue in codon 41 are GSK3 β phosphorylation sites.

KAD rat harbored a nonsense mutation resulting in the truncated APC protein (Δ 2523), in which the β -catenin-binding region was retained. The KAD rat was viable and showed the normal distribution of β -catenin in colon epithelium and no spontaneous colon tumors. These findings suggested that Wnt signal might not be activated in the non-treated colon epithelium of KAD rats. In humans, a subset of attenuated familial adenomatous polyposis harbors C-terminal-truncated APC mutations such as Δ 2644 and Δ 2663.^(19,20) The Δ 2644 APC protein failed to activate Wnt signaling,⁽²¹⁾ and these patients are rarely related to the occurrence of colonic polyposis, but are responsible for the development of extracolonic lesions, including desmoids, gastric fundic gland hyperplastic polyposis, and osteomas. Although we have not yet observed such extracolonic lesions in the KAD rat, further examinations will allow us to establish the KAD rat as a model for attenuated familial adenomatous polyposis.

The AOM/DSS-treated KAD rat showed colon tumors in 100% incidence, much higher in multiplicity (~10-fold) and more advanced in malignancy than the control F344 rat. These tumors can be obtained in only a short period of 15 weeks. We therefore concluded that AOM/DSS colon carcinogenesis was extensively enhanced in the KAD rat. This carcinogenesis model has also several advantages over the Pirc rat model. The epithelial malignancy of our model is more significant than the Pirc model: our model could induce adenocarcinomas (multiplicity is 3.0 ± 0.9), whereas most tumors developed in the colon of the Pirc rat were adenomas. This suggests that we could obtain multiple colon tumors in a shorter period (<15 experimental weeks). Next, we can evaluate the effects of potential carcinogens on colon carcinogenesis more strictly, because KAD are free from spontaneous tumors. Additionally, we can prepare tumor-bearing animals in accordance with our needs, which is a major concern in practical studies. It has been thought that an ideal colon carcinogenesis model would involve not only the efficient induction of tumors but also similar tumor characteristics and good availability for clinical application. The colon tumors developed in the KAD rat showed a predominant distribution in the rectum and distal colon and the accumulation of β -catenin protein, similar to human CRC. Furthermore, the tumors induced were large enough to be observed by endoscopy and biopsied tumor specimens were successfully diagnosed. These findings indicate that the KAD colorectal carcinogenesis model has the potential to mimic clinical operations for human CRC. Our results described here strongly suggest that AOM/DSS-induced colon carcinogenesis with the KAD rat model is ideal and provides an excellent tool to investigate basic and clinical studies on colitis-related CRC. For example, this model enables efficient evaluation of the effects of novel anticancer drugs on tumor regression as well as the effects of anti-inflammatory agents on tumor development. Combination with recently devel-

oped fluorescence probes that image viable cancer cells⁽²²⁾ would provide clearer images of tumors and further insights into the pathogenesis of CRC.

In contrast with the AOM/DSS-treated KAD rats, neither AOM-treated nor DSS-treated KAD rats developed colon tumors. It is well known that no colon tumors occurred in the AOM-treated or DSS-treated F344 rats within as short as 15 weeks by the carcinogenesis test.^(7,23,24) All AOM/DSS-treated KAD rats developed colon tumors. They also had significant diarrhea for a few weeks after cessation of the DSS exposure. These findings indicate that the KAD rat is susceptible to inflammation provoked by a colitis-inducing agent, DSS, and suggest that severe inflammation of the colon epithelia might be involved in the enhancement of colon carcinogenesis in the KAD rat.

DSS-induced colitis occurs mainly in the distal colon,⁽²⁵⁾ which is consistent with the predominant distribution of tumors to the distal colon and rectum in the AOM/DSS-treated KAD rat. Additionally, no K-ras mutation was found in the tumors of AOM/DSS-treated KAD rats. K-ras mutation plays a role as a promoter through enhancing COX-2 and iNOS expression in the presence of inflammatory stimuli.⁽¹⁶⁾ However, it is likely that, in our model, DSS enabling the induction of severe inflammation might replace the K-ras mutation. In fact, no mutations of K-ras and a high incidence of substitutions of *Apc* and *p53* genes were found in the colonic tumors induced by a colonic carcinogen, DMH, and a colitis-inducing compound, trinitrobenzene sulfonic acid.⁽²⁶⁾ These findings may support our idea that inflammation provoked by DSS plays an important role in colon carcinogenesis in the KAD rat, and the C terminus of APC, which is lacking in the KAD rat, might be involved in the effect of DSS on tumor development.

The C terminus of APC, which is lacking in the KAD rat, comprises a 321-amino acid polypeptides and contains a part of the basic domain, EB1-binding domain, and PDZ domain,⁽²⁷⁾ by which APC interacts with a variety of cytoskeletal proteins, such as microtubules, the microtubule plus end binding protein (EB1), and the mammalian homolog of Discs large.⁽²⁸⁻³⁰⁾ With these domains, APC contributes directly and/or indirectly to cell migration, adhesion, chromosome segregation, spindle assembly, and apoptosis in the epithelium of the gut.^(31,32) In the DSS colitis model, microbiota alteration, epithelial cell toxicity, increased intestinal permeability, and macrophage activation have been proposed as potential pathogenesis mechanisms of colitis.^(33,34) Although so far there is no direct evidence linking these colitis pathogenesises to the functions of APC domains, it is expected that cell migration or adhesion occurring in response to DSS treatment might be disturbed in KAD by the lack of the C-terminal domains. Alternatively, the responses of epithelial cells to cytokines released from macrophages induced by DSS might be altered. Further pathophysiological analysis of the KAD rat colon epithelium would provide insights into the association of the C terminus of APC with colitis. Importantly, other rodent *Apc* mutant models, such as Min mice and Pirc rats, completely lose all protein interaction sites located in the C-terminal half of the protein. Thus, it is very difficult to determine whether the susceptibility to DSS-induced colitis would result from the effects of the C-terminal or central regions of APC.

In summary, we established an enhanced rat AOM/DSS-induced colitis-related colon carcinogenesis model using a novel *Apc* mutant KAD rat. This colon carcinogenesis model system, to our knowledge, is the most effective in the experimental induction of colon tumors and therefore will contribute greatly to promote experimental studies on the pathogenesis, prevention, and treatment of CRC. The KAD rat also provides insights into the involvement of the C terminus of APC in the development of colitis-related CRC.

Acknowledgments

The KAD rat strain (NBPR Rat No. 0443), whose official strain name is F344-*Apc*^{miKyo} is deposited in the National BioResource Project – Rat in Japan and is available from the Project (<http://www.anim.med.kyoto-u.ac.jp/nbr>). This work was supported in part by a Grant-in-aid for Cancer Research from the Ministry of Health, Labour, and Welfare and

Grants-in-Aid for Scientific Research from the Japan Society for the Promotion of Science (21300153 to TK) and Industrial Technology Research Grant Program in 2008 from New Energy and the Industrial Technology Development Organization (NEDO) of Japan. We are grateful to K. Kumafuji, S. Nakanishi, F. Tagami, and M. Yokoe for their excellent technical assistance.

References

- 1 WHO. WHO Media Center, Cancer, Fact sheet No. 297. Geneva: WHO, 2009.
- 2 Itzkowitz SH, Yio X. Inflammation and cancer IV. Colorectal cancer in inflammatory bowel disease: the role of inflammation. *Am J Physiol Gastrointest Liver Physiol* 2004; **287**: G7–17.
- 3 Rutter M, Saunders B, Wilkinson K *et al*. Severity of inflammation is a risk factor for colorectal neoplasia in ulcerative colitis. *Gastroenterology* 2004; **126**: 451–9.
- 4 Tanaka T, Kohno H, Suzuki R, Yamada Y, Sugie S, Mori H. A novel inflammation-related mouse colon carcinogenesis model induced by azoxymethane and dextran sodium sulfate. *Cancer Sci* 2003; **94**: 965–73.
- 5 Kohno H, Suzuki R, Sugie S, Tanaka T. β -Catenin mutations in a mouse model of inflammation-related colon carcinogenesis induced by 1,2-dimethylhydrazine and dextran sodium sulfate. *Cancer Sci* 2005; **96**: 69–76.
- 6 Tanaka T, Suzuki R, Kohno H, Sugie S, Takahashi M, Wakabayashi K. Colonic adenocarcinomas rapidly induced by the combined treatment with 2-amino-1-methyl-6-phenylimidazo[4,5-*b*]pyridine and dextran sodium sulfate in male ICR mice possess β -catenin gene mutations and increases immunoreactivity for β -catenin, cyclooxygenase-2 and inducible nitric oxide synthase. *Carcinogenesis* 2005; **26**: 229–38.
- 7 Onose J, Imai T, Hasumura M, Ueda M, Hirose M. Rapid induction of colorectal tumors in rats initiated with 1,2-dimethylhydrazine followed by dextran sodium sulfate treatment. *Cancer Lett* 2003; **198**: 145–52.
- 8 Tanaka T, Yasui Y, Tanaka M, Tanaka T, Oyama T, Rahman KMW. Melatonin suppresses AOM/DSS-induced large bowel oncogenesis in rats. *Chem Biol Interact* 2009; **177**: 128–36.
- 9 Kinzler KW, Nilbert MC, Su LK *et al*. Identification of FAP locus genes from chromosome 5q21. *Science* 1991; **253**: 661–5.
- 10 Suzui M, Okuno M, Tanaka T, Nakagama H, Moriwaki H. Enhanced colon carcinogenesis induced by azoxymethane in min mice occurs via a mechanism independent of beta-catenin mutation. *Cancer Lett* 2002; **183**: 31–41.
- 11 Tanaka T, Kohno H, Suzuki R *et al*. Dextran sodium sulfate strongly promotes colorectal carcinogenesis in *Apc*^{Min/+} mice: inflammatory stimuli by dextran sodium sulfate results in development of multiple colonic neoplasms. *Int J Cancer* 2006; **118**: 25–34.
- 12 Amos-Landgraf JM, Kwong LN, Kendzierski CM *et al*. A target-selected *Apc*-mutant rat kindred enhances the modeling of familial human colon cancer. *Proc Natl Acad Sci USA* 2007; **104**: 4036–41.
- 13 Mashimo T, Yanagihara K, Tokuda S *et al*. An ENU-induced mutant archive for gene targeting in rats. *Nat Genet* 2008; **40**: 514–15.
- 14 Imai Y, Inoue H, Kataoka A *et al*. Pael receptor is involved in dopamine metabolism in the nigrostriatal system. *Neurosci Res* 2007; **59**: 413–25.
- 15 Takahashi M, Fukuda K, Sugimura T, Wakabayashi K. β -catenin is frequently mutated and demonstrates altered cellular location in azoxymethane-induced rat colon tumors. *Cancer Res* 1998; **58**: 42–6.
- 16 Takahashi M, Wakabayashi K. Gene mutations and altered gene expression in azoxymethane-induced colon carcinogenesis in rodents. *Cancer Sci* 2004; **95**: 475–80.
- 17 Gohma H, Kuramoto T, Kuwamura M *et al*. WTC deafness Kyoto (*dfk*): a rat model for extensive investigations of *Kcnql* functions. *Physiol Genomics* 2006; **24**: 198–206.
- 18 Moser AR, Pitot HC, Dove WF. A dominant mutation that predisposes to multiple intestinal neoplasia in the mouse. *Science* 1990; **247**: 322–4.
- 19 Couture J, Mitri A, Lagace R *et al*. A germline mutation at the extreme 3' end of the APC gene results in a severe desmoid phenotype and is associated with overexpression of beta-catenin in the desmoid tumor. *Clin Genet* 2000; **57**: 205–12.
- 20 Matsubara N, Isozaki H, Tanaka N. The farthest 3' distal end APC mutation identified in attenuated adenomatous polyposis coli with extracolonic manifestations. *Dis Colon Rectum* 2000; **43**: 720–1.
- 21 Morin PJ, Sparks AB, Korinek V *et al*. Activation of β -catenin-Tcf signaling in colon cancer by mutations in β -catenin or APC. *Science* 1997; **275**: 1787–90.
- 22 Urano Y, Asanuma D, Hama Y *et al*. Selective molecular imaging of viable cancer cells with pH-activatable fluorescence probes. *Nat Med* 2009; **15**: 104–9.
- 23 Ghirardi M, Nascimbeni R, Villanacci V, Fontana MG, Di Betta E, Salerni B. Azoxymethane-induced aberrant crypt foci and colorectal tumors in F344 rats: sequential analysis of growth. *Eur Surg Res* 1999; **31**: 272–80.
- 24 Paulsen JE, Loberg EM, Olstorn HB, Knutsen H, Steffensen IL, Alexander J. Flat dysplastic aberrant crypt foci are related to tumorigenesis in the colon of azoxymethane-treated rat. *Cancer Res* 2005; **65**: 121–9.
- 25 Okayasu I, Hatakeyama S, Yamada M, Ohkusa T, Inagaki Y, Nakaya R. A novel method in the induction of reliable experimental acute and chronic ulcerative colitis in mice. *Gastroenterology* 1990; **98**: 694–702.
- 26 Santiago C, Pagan B, Isidro AA, Appleyard CB. Prolonged chronic inflammation progresses to dysplasia in a novel rat model of colitis-associated colon cancer. *Cancer Res* 2007; **67**: 10 766–73.
- 27 Aoki K, Taketo MM. Adenomatous polyposis coli (APC): a multi-functional tumor suppressor gene. *J Cell Sci* 2007; **120**: 3327–35.
- 28 Munemitsu S, Souza B, Muller O, Albert I, Rubinfeld B, Polakis P. The APC gene product associates with microtubules *in vivo* and promotes their assembly *in vitro*. *Cancer Res* 1994; **54**: 3676–81.
- 29 Su LK, Burrell M, Hill DE *et al*. APC binds to the novel protein EB1. *Cancer Res* 1995; **55**: 2972–7.
- 30 Matsumine A, Ogai A, Senda T *et al*. Binding of APC to the human homolog of the *Drosophila* discs large tumor suppressor protein. *Science* 1996; **272**: 1020–3.
- 31 McCartney BM, Nathke IS. Cell regulation by the Apc protein: Apc as master regulator of epithelia. *Curr Opin Cell Biol* 2008; **20**: 186–93.
- 32 Hanson CA, Miller JR. Non-traditional roles for the adenomatous polyposis coli (APC) tumor suppressor protein. *Gene* 2005; **361**: 1–12.
- 33 Boismenu R, Chen Y. Insights from mouse models of colitis. *J Leukoc Biol* 2000; **67**: 267–78.
- 34 Elson CO, Cong Y, McCracken VJ, Dimmitt RA, Lorenz RG, Weaver CT. Experimental models of inflammatory bowel disease reveal innate, adaptive, and regulatory mechanisms of host dialogue with the microbiota. *Immunol Rev* 2005; **206**: 260–76.

Supporting Information

Additional supporting information may be found in the online version of this article:

Fig. S1. Signet-ring cell carcinoma observed in the colon of AOM/DSS-treated KAD rats. Four signet-ring cell carcinomas were observed in AOM/DSS-treated KAD rats (group 1).

Fig. S2. Endoscopic observation of KAD colon tumors and biopsy. (A) Endoscopic image of a colon tumor in a KAD rat at week 11. Bleeding from this tumor was found (arrow). (B) Development of colorectal lesions in KAD rats treated with AOM and DSS (group 1). The average numbers of lesions observed by endoscopy were plotted. (C) Microscopic view of a specimen biopsied under endoscopic observation. The specimen was diagnosed as well-differentiated adenocarcinoma. Bar: 60 μ m.

Video S1. Biopsy of a colorectal tumor induced by AOM/DSS two-stage colitis-related carcinogenesis in the KAD rat.

Table S1. Primers used in screening for *Apc* mutation in KURMA ENU-mutagenized DNA archives.

Please note: Wiley-Blackwell are not responsible for the content or functionality of any supporting materials supplied by the authors. Any queries (other than missing material) should be directed to the corresponding author for the article.

—Review—

Review Series: Animal Bioresource in Japan

National BioResource Project-Rat and Related Activities

Tadao SERIKAWA, Tomoji MASHIMO, Akiko TAKIZAWA, Ryoko OKAJIMA, Naoki MAEDOMARI, Kenta KUMAFUJI, Fumi TAGAMI, Yuki NEODA, Mito OTSUKI, Satoshi NAKANISHI, Ken-ichi YAMASAKI, Birger VOIGT, and Takashi KURAMOTO

*Institute of Laboratory Animals, Graduate School of Medicine, Kyoto University,
Sakyo-ku, Kyoto 606-8501, Japan*

Abstract: In order to establish a system to facilitate the systematic collection, preservation, and provision of laboratory rats (*Rattus norvegicus*) and their derivatives, the National BioResource Project-Rat (NBRP-Rat) was launched in July 2002. By the end of 2008, more than 500 rat strains had been collected and preserved as live animals, embryos, or sperm. These rat resources are supplied to biomedical scientists in Japan as well as in other countries. This review article introduces NBRP-Rat and highlights the phenome project, recombinant inbred strains, BAC clone libraries, and the ENU-mutant archive, named the Kyoto University Rat Mutant Archive (KURMA). The future direction of rat resources are also discussed.

Key words: bioresource, ENU mutagenesis, NBRP-Rat, phenome project, RI strains

History of Laboratory Rats

In Japan, the first appearance of rat (*Rattus norvegicus*) domestication was seen in two guides for breeding fancy rodents, rats and mice, published around 1780. The works *Yosotamanokakehashi* from 1775 (see Fig. 1) and *Chingansodategusa* from 1787 [24, 26] introduced coat color variants of fancy rodents and explained their breeding, feeding, and housing. In Europe, rat domestication began in the 1800s when rat baiting was developed as a sport, and albino rats were observed occasionally and utilized for entertainment or breeding purposes [3].

The rat began its career as a laboratory animal in Europe in the 1850s, and became the first mammalian species to be domesticated for scientific purposes [12]. Their suitable size and easy handling might have been

the major selective points in early animal experiments in the studies of breeding, behavior, psychology, nutrition, endocrinology, genetics, and others. Rats are now well known as the most important animals for safety or toxicological testing of chemical compounds, including drug candidates. Laboratory rats derived from ‘outbred’ or ‘closed colony’ animals, like Wistar or Sprague-Dawley rats, are usually supplied by commercial breeders and used for such testing, although inbred strains, such as Fischer (F344) or Long Evans (LE), are also popularly used for similar purposes. Some 700 different rat strains that comprise the above mentioned inbred and outbred strains of various natures (spontaneous mutant, congenic, recombinant inbred, consomic, transgenic, etc.) have recently become available through resource centers, and the majority have been developed from only a few founder strains, of which the Wistar strain plays

(Received 11 March 2009 / Accepted 19 May 2009)

Address corresponding: T. Serikawa, Institute of Laboratory Animals, Graduate School of Medicine, Kyoto University, Sakyo-ku, Kyoto 606-8501, Japan

supplied to other institutions, beginning in 1911.

Many reference strains and model rats have been developed in Japan from imported outbred rats from the USA, especially from the Wistar Institute or commercially available Wistar rats and Sprague-Dawley rats or Long-Evans rats. Spontaneously hypertensive rats (SHR) [19] and stroke-prone hypertensive rats (SHRSP) [20] were developed from Wistar rats at Kyoto University (Kyo:Wistar rats) and are representative rat models of human diseases. Furthermore, many genetic models of human diseases have been developed by selective breeding methods in Japan and other countries; for instance, Helen Dean King not only developed the Wistar-derived inbred strain King Albino (PA or WKA), but also captured wild rats to produce inbred strains and succeeded in developing the BN strain. Many inbred strains were also independently developed at Columbia University: F344, AUG, COP, and at other universities and institutes [12].

The laboratory rat is now widely used for translational research, because it is a suitable animal for medical experiments due to its well-characterized physiology and not least because it is large enough for many surgical manipulations and examinations that cannot be performed on mice. To understand the genetic base of rat models, the first whole genetic map of the rat was drawn using simple sequence polymorphism (SSLP) markers in 1992 [23] and the whole draft sequence of the rat genome was reported in 2004 [6]. Recent developments, such as the establishment of rat ES or iPS cells or the generation of gene-knockout rats using Zinc Finger Nucleases (ZFN), will boost the utilization of rats, especially in the field of functional genomics [4, 10, 11, 16].

Rat Bio Resource Centers

Important rat strains for various research fields in life science have been maintained for more than 100 years on the basis of individual efforts by many scientists. Such effort is intrinsically inefficient and susceptible to unexpected changes in funding and local interests. The NIH rat model repository workshop was held in August 1998, and 58 scientists from the USA and elsewhere discussed the needs, use, opportunities, and parameters

for optimal importation, standardization, maintenance, and distribution of genetically defined rat strains. The group of internationally recognized scientists strongly encouraged the NIH to establish a national rat genetics resource center. As a result, the Rat Resource Research Center (RRRC) was established in 2001. A similar approach on a larger scale was undertaken in Japan in 2002 with the National BioResource Project-Rat, (NBRP-Rat), addressing the need of collecting, preserving, and supplying unique rat strains that resemble human diseases or are of other value for biomedical research, and which have mainly been developed in Japan. These two large rat repositories, RRRC and NBRP-Rat, are operating internationally [2].

National BioResource Project-Rat (NBRP-Rat)

The aims of the National BioResource Project-Rat (NBRP-Rat) are the collection of rat strains, phenotypic and genetic characterization, the maintenance of live stock under specific-pathogen free conditions, the cryo-preservation of embryos and sperm [8, 18], the preparation and maintenance of a publicly accessible database on deposited rat strains (<http://www.anim.med.kyoto-u.ac.jp/NBR/>), and the global supply of these rat strains. The NBRP-Rat is a very timely project in this field and we could elevate the potential of rat resources by performing this fundamental project as described below [24].

By the end of 2008, more than 500 rat strains had been deposited in the NBRP-Rat. Inbred strains, substrains, and congenic strains are major collections. In the genetic categories, animal models for human diseases or mutant strains developed from rats with spontaneous mutations or by selective breeding for particular phenotypes are included. Recombinant inbred strains and consomic strains are also preserved in the NBRP-Rat repository. Reporter gene transgenic rats are useful tools for investigating the physiological or pathological process in animal models. Transgenic rats with GFP, LacZ, and DsRed are particularly valuable for examining cellular fate in living animals [22], and have great potential utility for cell trafficking studies after organ and cell transplantations. Tissue organogenesis and trans-differentiation of stem cells are expected to be targets of study

using these reporter gene transgenic rats. In addition to the rat strains, a set of sperm and DNA of 5,000 ENU mutagenized F344 G1 animals have been placed in the NBRP repository [15].

Rat strains or their DNA samples have been supplied to 466 institutions in Japan and 22 institutions in the USA, Canada, UK, Germany, Sweden, Thailand, Indonesia, Malaysia, China, and Taiwan. To support the standardization and ease the exchange of cryopreserved rat bioresources among research and resource laboratories worldwide, two DVDs (Japanese and English versions), which contain protocols and movies of the cryopreservation of rat embryos and sperm, intracytoplasmic sperm injection, and re-derivation techniques, have been produced and supplied to the research community.

Phenome Project

To re-evaluate the collected strains at NBRP-Rat, male rats of 163 inbred strains and female rats of 40 inbred strains have been phenotypically characterized for 109 parameters under the Rat Phenome Project [13]. This systematic characterization is the first large-scale strain survey of many phenotypes of biological importance in the rat. In this project, 179 rat strains (including wild rats) have also been genotyped with 357 microsatellite markers [14]. In the European STAR project, 96 rat strains from NBRP characterized in the phenome project have been genotyped with approximately 20,000 SNPs [21].

Phenotype data have been collected for 7 categories, functional observational battery (neurobehavior), behavior studies, blood pressure, biochemical blood tests, hematology, urology, and anatomy, which include 109 parameters. A major feature of this phenome project is the development of phenotypic 'Strain Ranking', which allows visual data scoring, shows the biological range of various phenotypic parameters, and reveals normal and abnormal values for various rat strains. 'Strain Ranking' at NBRP-Rat provides an opportunity to easily and simultaneously compare phenotypic values for multiple rat strains, and could reveal unique and unknown characteristics even in well-characterized strains. For instance, strain ranking in the passive avoidance test identified the unique learning ability of BN strains,

whose DNA was used for the Rat Genome Project.

Female data have recently been added and it is now possible to display gender differences (Fig. 2). The examples impressively demonstrate that glucose, triglyceride, and hematocrit values are significantly higher in males. In contrast, MCHC, prothrombin, plasma chloride, and relative adrenal weights show significantly higher values in females. Although comparative evaluations of these gender differences in rats and humans or other laboratory animals have not been completed yet, important rats were identified by this project. Phenome data are publicly available from our website (<http://www.anim.med.kyoto-u.ac.jp/NBR/phenome.aspx>).

NBRP-Rat is also genotyping selected rat strains and has developed a pedigree which integrates all major rat strains as well as several mutants and even wild rats from different continents (<http://www.anim.med.kyoto-u.ac.jp/NBR/phylo.aspx>). The genotyping comprises 357 microsatellite markers and includes animals from some 180 different origins. Furthermore, a charting tool utilizes these data to draw strain-specific phylogenetic charts that refer to a freely selectable rat strain. These useful tools and data support investigators in elucidating the phylogenetic relationships of rat strains and to select suitable strains for genetic experiments.

Functional Polymorphisms

An allelic variation that cause changes in the appearance of any possible phenotype, such as enzyme activity, disease susceptibility etc. is called a functional polymorphism. NBRP-Rat has recently surveyed 140 rat strains for gene mutations reported in particular rat strains that are responsible for functional polymorphisms (Fig. 3) [9]. Forty-nine rat strains show the insertion type of *Cdkn1a/p21* [29], suggesting their resistance to prostate cancer; 79 rat strains have the duplication type of *Fcgr3* [1], suggesting their resistance to experimentally induced nephritis; and 63 and 29 rat strains have point mutations of *Lss* and *Fdft1* [17], respectively, suggesting their susceptibility to cataracts. Point mutations of *Gpr10* type [28] could be detected in 45 strains, suggesting their tendency toward overeating; certainly, body weight values at 10 weeks of age were significantly higher in this group. Such information is very helpful

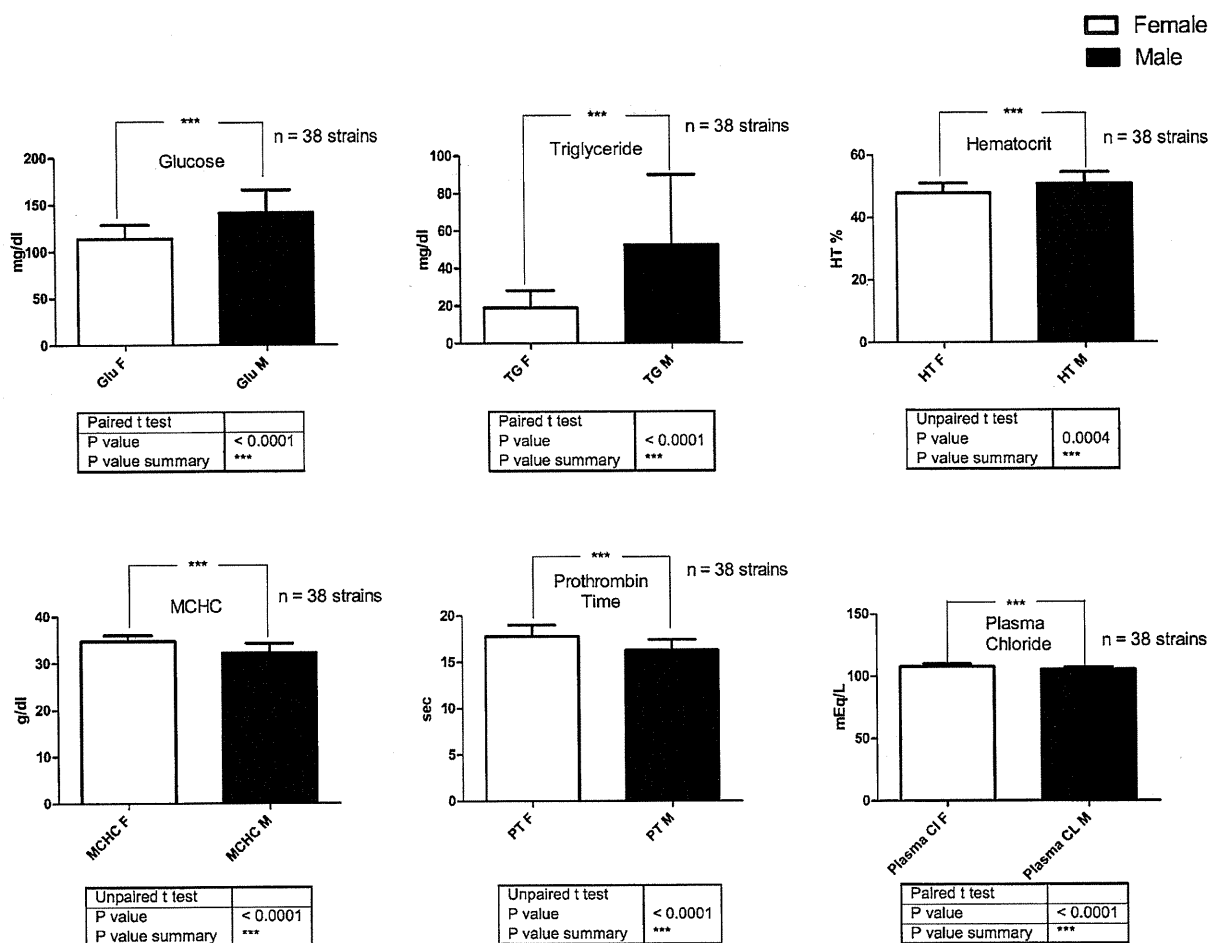


Fig. 2. Gender differences of serum biochemical and hematological parameters in rat inbred strains.

for selecting suitable rat strains for particular experiments. Since functional polymorphisms were also found in outbred or closed colonies at different rates among rat colonies [9], we recommend that testing or experiments with rats should be planned after giving careful consideration to this issue.

Recombinant Inbred Strains

Recombinant inbred (RI) strains are produced from an outcross between two well-characterized inbred strains followed by at least 20 generations of inbreeding to create several new inbred lines with a genome that is a mosaic of the parental genomes. The resulting RI strains are independent inbred strains with unique phenotypes

due to the allelic mixture of the parental genes. Once the fully inbred status has been achieved, the results of a single genotyping of strain distribution patterns (SDPs) of polymorphic genetic markers, can be utilized in all future experiments. In subsequent projects, only the phenotype of the RI strains needs to be determined and can be linked to the stable genomic information. Furthermore, RI strains provide a suitable genetic platform for quantitative trait locus (QTL) analysis by reducing individual, environmental, and measurement variability.

The largest rat RI strain panel is available from NBRP-Rat. The LEXF/FXLE RI set (n=34), derived by reciprocal crossing of F344/Stm and LE/Stm [25], has been genotyped for approximately 20,000 SNPs and pheno-

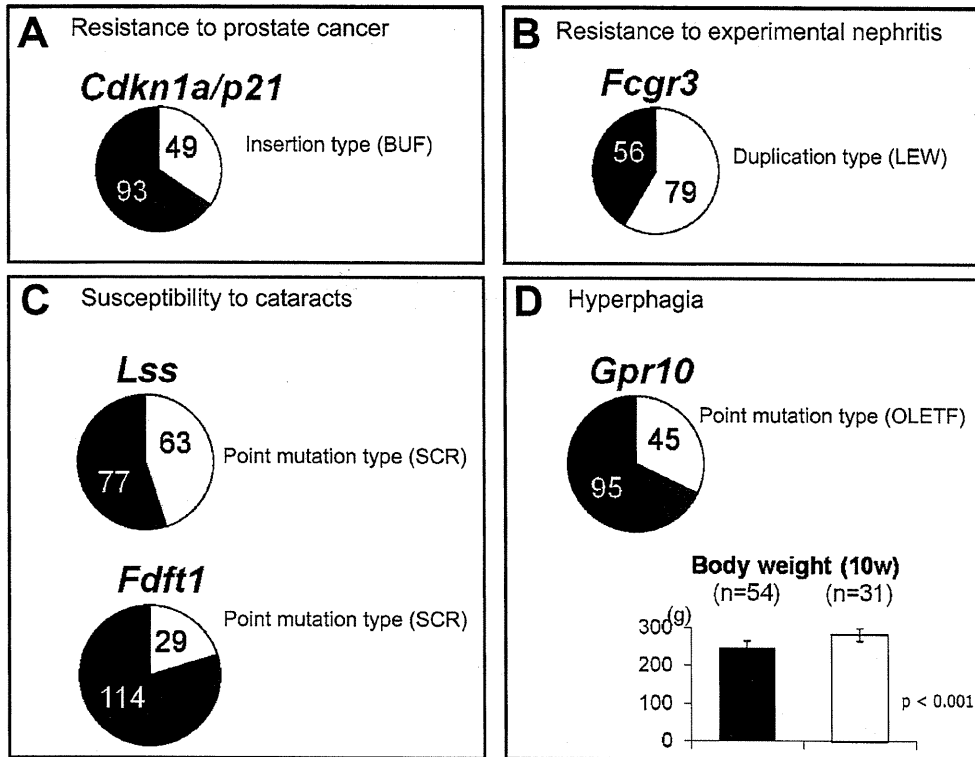


Fig. 3. Distribution of disease-related functional polymorphisms in rat inbred strains. (A) Insertional mutation in the promoter region of the *Cdkn1a* gene is associated with resistance to prostate cancer. (B) Duplication of the *Fcgr3* gene is associated with resistance to experimentally induced nephritis. (C) Missense mutations of *Lss* and *Fdft1* genes are associated with susceptibility to cataracts. (D) Missense mutation at the translation initiation codon of the *Gpr10* gene is associated with hyperphagia. The average body weight of the mutant-type strains ($n=31$) is significantly higher than that of wild-type strains ($n=54$).

typed for 74 quantitative traits. QTL analysis has already detected 250 QTLs for these traits, indicating the usefulness of the LEXF/FXLE to identify QTLs [21, 27].

Rat BAC Clone Libraries

To strengthen the power of the LEXF/FXLE RI strain, BAC libraries with ten-fold coverage were constructed for the parent F344/Stm (238,080 clones, average length 116 kb) and LE/Stm strains (259,968 clones, average length 129 kb), as a collaboration with RIKEN Genomic Sciences Center and the National Institute of Genetics. All BAC clones were deposited at the Gene Engineering Division, RIKEN BioResource Center to enable their worldwide distribution. BAC ends were sequenced and mapped to the reference genome sequence of the BN

strain. In the F344/Stm BAC library, 155,144 clones were mapped, of which 138,800 (89%) clones were mapped with both ends and 16,344 (11%) with one of either ends. The mapped F344/Stm BAC clones cover ~96% of autosomes and ~92% of the X chromosome. In the LE/Stm BAC library, 103,062 clones were mapped, of which 55,821 (54%) clones were mapped with both ends and 47,241 (46%) with one of either ends. The mapped LE/Stm BAC clones cover ~82% of autosomes and ~52% of the X chromosome. Mapping data can be accessed publicly using the GBrowser at the homepage of NBRP-Rat (<http://analysis2.lab.nig.ac.jp/ratBrowser/cgi-bin/index.cgi?org=rn>).

Table 1. Generation of gene-targeted rats from KURMA

Gene	Screening on KURMA by MuT-POWER					Recovery by ICSI			
	Number of G1 samples screened	Mbp screened	Mutations found	Mutation type	Mutations per Mb	Injected oocytes	Transferred oocytes (%)*	Born (%)	Mutated
Gene A	1,536	12.50	A → C	E → A (Missense)	6.25	36	30 (83.3)	9 (25.0)	6 (♂4, ♀2)
			A → C	N → H (Missense)					
Gene B	1,536	4.22	C → A	S → X (Nonsense)	4.22	37	30 (81.1)	10 (27.0)	3 (♂1, ♀2)
Gene C	1,536	6.45	A → T	Q → L (Missense)	2.15	282	240 (85.1)	22 (7.8)	9 (♂4, ♀5)
			A → T	K → M (Missense)					
			T → C	Silence					
Gene D	4,608	16.92	T → G	L → R (Missense)	8.46	97	75 (77.3)	11 (11.3)	7 (♂2, ♀5)
			T → C	Silence					
Gene E	4,608	14.32	T → A	L → Q (Missense)	7.16	203	156 (76.8)	17 (8.4)	10 (♂4, ♀6)
			G → A	Intronic					
Total 5 genes	–	54.11	10	–	5.41	693	566 (81.7)	84 (12.1)	40 (♂17, ♀23)

*: The 2-cell cleaved embryos were transferred into the oviducts of pseudopregnant F344/NSlc rats.

Kyoto University Rat Mutant Archive (KURMA)

Although the laboratory rat is an increasingly used mammalian model in biomedical research, there was no simple technology for producing *in vivo* genetically engineered mutations equivalent to knockout or knock-in mice for several decades. To overcome such a limitation, we have generated a large repository of ENU-induced mutations, called the Kyoto University Rat Mutant Archive (KURMA) [15]. DNA mutations in the repository can be efficiently screened with a high-throughput and low-cost assay based on the Mu-transposition reaction (MuT-POWER). Animals carrying any mutations can be recovered from frozen sperm by intracytoplasmic sperm injection (ICSI). Table 1 shows the results of screening by MuT-POWER for particular target genes and the recovery of mutated rats by ICSI, which indicates the reliability of these technologies for establishing gene-targeted rat models from the KURMA. There are estimated to be 2.5–3.5 millions mutations in the KURMA, which means that at least one mutation of the particular gene will be acquired from 5,000 samples. Expansion up to 10,000 male G1 samples would guarantee mutations in any gene of interest.

The KURMA has enabled the production of several rat models for human diseases, including epilepsy, cancer, hypertension, or diabetes, a series of diseases for which mice have proved less interesting. With such a

variety of mutations in different genetic contexts, the teaching of comparative pathology and functional genomics will increase.

Future Aspects of Rat Resource Center

The major aim of rat resource centers is the supply of bio materials to the research community. Progressing technologies require existing repositories to preserve and maintain not only animals or materials of traditionally derived rat strains but also genetically engineered rats. ENU- or transposon-mediated mutagenized archives with thousands of individual samples have to be stored and made available in the interests of biomedical research. Powerful genetic manipulations of rat ES cells [4, 10], iPS cells [11], or other techniques enable the generation of knock-out models and will greatly expand the scope of present experimental limitations with new rat resources. Such repositories would ideally be managed across core centers in the USA, EU, and Japan to share the resources and standardize cryopreservation technologies. In these centers, laboratory space and equipment along with rat strains and related materials, should be provided to interested researchers to perform preliminary experiments and for archive screening. The advantage of bioresources in combination with sophisticated technologies, such as MRI, other bio-imaging technologies, behavioral measure stations, etc. is the

acquisition of fast and accurate results as prerequisites for larger projects.

Acknowledgment(s)

NBRP-Rat was implemented by the Ministry of Education, Culture, Sports, Science and Technology, Japan. We thank the collaborators in NBRP-Rat, K. Kitada at Hokkaido University, E. Kobayashi and Y. Hakamata at Jichi Medical University, Y. Obata and A. Yoshiki at RIKEN BRC, M. Hirabayashi at the National Institute of Natural Science, K. Hioki and T. Etoh at the Central Institute of Experimental Animals, K. Komeda at Tokyo Medical University, R. Hokao at the Institute for Animal Reproduction, T. Nishimori and H. Tutumi at Nissei BIRIS, K. Matsumoto at Tokushima University, and T. Nabika at Shimane University. We also thank A. Toyoda for providing statistical information on BAC clone libraries.

Creation of the KURMA was supported in part by Grants-in-aid for Scientific Research from the Japan Society for the Promotion of Science, a Grant-in-aid for Cancer Research from the Ministry of Health, Labour and Welfare, and the Industrial Technology Research Grant Program in 2008 from the New Energy and Industrial Technology Development Organization (NEDO) of Japan.

References

- Aitman, T.J., Dong, R., Vyse, T.J., Norsworthy, P.J., Johnson, M.D., Smith, J., Mangion, J., Robertson-Lowe, C., Marshall, A.J., Petretto, E., Hodges, M.D., Bhargal, G., Patel, S.G., Sheehan-Rooney, K., Duda, M., Cook, P.R., Evans, D.J., Domin, J., Flint, J., Boyle, J.J., Pusey, C.D., and Cook, H.T. 2006. Copy number polymorphism in *Fcgr3* predisposes to glomerulonephritis in rats and humans. *Nature* 439: 851–855.
- Aitman, T.J., Critser, J.K., Cuppen, E., Dominiczak, A., Fernandez-Suarez, X.M., Flint, J., Gauguier, D., Geurts, A.M., Gould, M., Harris, P.C., Holmdahl, R., Hubner, N., Izsvak, Z., Jacob, H.J., Kuramoto, T., Kwitek, A.E., Marrone, A., Mashimo, T., Moreno, C., Mullins, J., Mullins, L., Olsson, T., Pravenec, M., Riley, L., Saar, K., Serikawa, T., Shull, J.D., Szpirer, C., Twigger, S.N., Voigt, B., and Worley, K. 2008. Progress and prospects in rat genetics: a community view. *Nat. Genet.* 40: 516–522.
- Boakes, R. 2008. Comparative psychology and beginning of behaviourism. pp. 136–175. *In: From Darwin to Behaviourism, Psychology and the Minds of Animals* (Boakes, R. ed.), Cambridge University Press, Cambridge.
- Buehr, M., Meek, S., Blair, K., Yang, J., Ure, J., Silva, J., McLay, R., Hall, J., Ying, Q.L., and Smith, A. 2008. Capture of authentic embryonic stem cells from rat blastocysts. *Cell* 135: 1287–1298.
- Donaldson, H.H. 1925. Research at the Wistar Institute, 1905–1925. *Science* 61: 480–483.
- Gibbs, R.A., Weinstock, G.M., Metzker, M.L., Muzny, D.M., Sodergren, E.J., Scherer, S., Scott, G., Steffen, D., Worley, K.C., Burch, P.E., Okwuonu, G., Hines, S., Lewis, L., DeRamo, C., Delgado, O., Dugan-Rocha, S., Miner, G., Morgan, M., Hawes, A., Gill, R., Celera, Holt, R.A., Adams, M.D., Amanatides, P.G., Baden-Tillson, H., Barnstead, M., Chin, S., Evans, C.A., Ferreira, S., Fosler, C., Glodek, A., Gu, Z., Jennings, D., Kraft, C.L., Nguyen, T., Pfannkoch, C.M., Sitter, C., Sutton, G.G., Venter, J.C., Woodage, T., Smith, D., Lee, H.M., Gustafson, E., Cahill, P., Kana, A., Doucette-Stamm, L., Weinstock, K., Fechtel, K., Weiss, R.B., Dunn, D.M., Green, E.D., Blakesley, R.W., Bouffard, G.G., De Jong, P.J., Osoegawa, K., Zhu, B., Marra, M., Schein, J., Bosdet, I., Fjell, C., Jones, S., Krzywinski, M., Mathewson, C., Siddiqui, A., Wye, N., McPherson, J., Zhao, S., Fraser, C.M., Shetty, J., Shatsman, S., Geer, K., Chen, Y., Abramzon, S., Nierman, W.C., Havlak, P.H., Chen, R., Durbin, K.J., Egan, A., Ren, Y., Song, X.Z., Li, B., Liu, Y., Qin, X., Cawley, S., Worley, K.C., Cooney, A.J., D'Souza, L.M., Martin, K., Wu, J.Q., Gonzalez-Garay, M.L., Jackson, A.R., Kalafus, K.J., McLeod, M.P., Milosavljevic, A., Virk, D., Volkov, A., Wheeler, D.A., Zhang, Z., Bailey, J.A., Eichler, E.E., Tuzun, E., Birney, E., Mongin, E., Ureta-Vidal, A., Woodwark, C., Zdobnov, E., Bork, P., Suyama, M., Torrents, D., Alexandersson, M., Trask, B.J., Young, J.M., Huang, H., Wang, H., Xing, H., Daniels, S., Gietzen, D., Schmidt, J., Stevens, K., Vitt, U., Wingrove, J., Camara, F., Mar Alba, M., Abril, J.F., Guigo, R., Smit, A., Dubchak, I., Rubin, E.M., Couronne, O., Poliakov, A., Hubner, N., Ganten, D., Goesele, C., Hummel, O., Kreitler, T., Lee, Y.A., Monti, J., Schulz, H., Zimdahl, H., Himmelbauer, H., Lehrach, H., Jacob, H.J., Bromberg, S., Gullings-Handley, J., Jensen-Seaman, M.I., Kwitek, A.E., Lazar, J., Pasko, D., Tonellato, P.J., Twigger, S., Ponting, C.P., Duarte, J.M., Rice, S., Goodstadt, L., Beatson, S.A., Emes, R.D., Winter, E.E., Webber, C., Brandt, P., Nyakatura, G., Adetobi, M., Chiaromonte, F., Elnitski, L., Eswara, P., Hardison, R.C., Hou, M., Kolbe, D., Makova, K., Miller, W., Nekrutenko, A., Riemer, C., Schwartz, S., Taylor, J., Yang, S., Zhang, Y., Lindpaintner, K., Andrews, T.D., Caccamo, M., Clamp, M., Clarke, L., Curwen, V., Durbin, R., Eyas, E., Searle, S.M., Cooper, G.M., Batzoglou, S., Brudno, M., Sidow, A., Stone, E.A., Venter, J.C., Payseur, B.A., Bourque, G., Lopez-Otin, C., Puente, X.S., Chakrabarti, K., Chatterji, S., Dewey, C., Pachter, L., Bray, N., Yap, V.B., Caspi, A., Tesler, G., Pevzner, P.A., Haussler, D., Roskin, K.M., Baertsch, R., Clawson, H., Furey, T.S., Hinrichs, A.S., Karolchik, D., Kent, W.J., Rosenbloom, K.R., Trumbower, H., Weirauch, M., Cooper, D.N., Stenson, P.D., Ma, B., Brent, M., Arumugam, M., Shteynberg, D., Copley, R.R., Taylor, M.S.,

- Riethman, H., Mudunuri, U., Peterson, J., Guyer, M., Felsenfeld, A., Old, S., Mockrin, S., and Collins, F. 2004. Genome sequence of the Brown Norway rat yields insights into mammalian evolution. *Nature* 428: 493–521.
7. Hatai, S. 1912. On the appearance of albino mutants in litters of the common norway rat, *Mus norvegicus*. *Science* 35: 875–876.
 8. Kashiwazaki, N., Seita, Y., Naoi, K., Takizawa, A., Kuramoto, T., and Serikawa, T. 2007. Generation of rat offspring derived from cryopreserved spermatozoa in Japanese National Bioresources. *Reprod. Fertil. Dev.* 19: 124–125.
 9. Kuramoto, T., Nakanishi, S., and Serikawa, T. 2008. Functional polymorphisms in inbred rat strains and their allele frequencies in commercially available outbred stocks. *Physiol. Genomics* 33: 205–211.
 10. Li, P., Tong, C., Mehrian-Shai, R., Jia, L., Wu, N., Yan, Y., Maxson, R.E., Schulze, E.N., Song, H., Hsieh, C.L., Pera, M.F., and Ying, Q.L. 2008. Germline competent embryonic stem cells derived from rat blastocysts. *Cell* 135: 1299–1310.
 11. Liao, J., Cui, C., Chen, S., Ren, J., Chen, J., Gao, Y., Li, H., Jia, N., Cheng, L., Xiao, H., and Xiao, L. 2009. Generation of induced pluripotent stem cell lines from adult rat cells. *Cell Stem Cell* 4: 11–15.
 12. Lindsey, J.R. 1979. Historical foundations. pp. 1–36. *In: The Laboratory Rat Volume I, Biology and Diseases* (Baker, H.J., Lindsey, J.R., and Weisbroth, S.H. eds.), Elsevier Academic Press, Boston.
 13. Mashimo, T., Voigt, B., Kuramoto, T., and Serikawa, T. 2005. Rat Phenome Project: the untapped potential of existing rat strains. *J. Appl. Physiol.* 98: 371–379.
 14. Mashimo, T., Voigt, B., Tsurumi, T., Naoi, K., Nakanishi, S., Yamasaki, K., Kuramoto, T., and Serikawa, T. 2006. A set of highly informative rat simple sequence length polymorphism (SSLP) markers and genetically defined rat strains. *BMC Genet.* 7: 19.
 15. Mashimo, T., Yanagihara, K., Tokuda, S., Voigt, B., Takizawa, A., Nakajima, R., Kato, M., Hirabayashi, M., Kuramoto, T., and Serikawa, T. 2008. An ENU-induced mutant archive for gene targeting in rats. *Nat. Genet.* 40: 514–515.
 16. Meng, X., Noyes, M.B., Zhu, L.J., Lawson, N.D., and Wolfe, S.A. 2008. Targeted gene inactivation in zebrafish using engineered zinc-finger nucleases. *Nat. Biotechnol.* 26: 695–701.
 17. Mori, M., Sawashita, J., and Higuchi, K. 2007. Functional polymorphisms of the *Lss* and *Fdft1* genes in laboratory rats. *Exp. Anim.* 56: 93–101.
 18. Nakatsukasa, E., Kashiwazaki, N., Takizawa, A., Shino, M., Kitada, K., Serikawa, T., Hakamata, Y., Kobayashi, E., Takahashi, R., Ueda, M., Nakashima, T., and Nakagata, N. 2003. Cryopreservation of spermatozoa from closed colonies, and inbred, spontaneous mutant, and transgenic strains of rats. *Comp. Med.* 53: 639–641.
 19. Okamoto, K. and Aoki, K. 1963. Development of a strain of spontaneously hypertensive rats. *Jpn. Circ. J.* 27: 282–293.
 20. Okamoto, K., Yamori, Y., and Nagaoka, A. 1974. Establishment of stroke-prone spontaneously hypertensive rat (SHR). *Circ. Res.* 34 and 35: 145–153.
 21. Saar, K., Beck, A., Bihoreau, M.T., Birney, E., Brocklebank, D., Chen, Y., Cuppen, E., Demonchy, S., Dopazo, J., Flicek, P., Foglio, M., Fujiyama, A., Gut, I.G., Gauguier, D., Guigo, R., Guryev, V., Heinig, M., Hummel, O., Jahn, N., Klages, S., Kren, V., Kube, M., Kuhl, H., Kuramoto, T., Kuroki, Y., Lechner, D., Lee, Y.A., Lopez-Bigas, N., Lathrop, G.M., Mashimo, T., Medina, I., Mott, R., Patone, G., Perrier-Cornet, J.A., Platzer, M., Pravenec, M., Reinhardt, R., Sakaki, Y., Schilhabel, M., Schulz, H., Serikawa, T., Shikhagaie, M., Tatsumoto, S., Taudien, S., Toyoda, A., Voigt, B., Zelenika, D., Zimdahl, H., and Hubner, N. 2008. SNP and haplotype mapping for genetic analysis in the rat. *Nat. Genet.* 40: 560–566.
 22. Sato, Y., Igarashi, Y., Hakamata, Y., Murakami, T., Kaneko, T., Takahashi, M., Seo, N., and Kobayashi, E. 2003. Establishment of Alb-DsRed2 transgenic rat for liver regeneration research. *Biochem. Biophys. Res. Commun.* 311: 478–481.
 23. Serikawa, T., Kuramoto, T., Hilbert, P., Mori, M., Yamada, J., Dubay, C.J., Lindpainter, K., Ganten, D., Guenet, J.L., Lathrop, G.M., and Beckmann, J.S. 1992. Rat gene mapping using PCR-analyzed microsatellites. *Genetics* 131: 701–721.
 24. Serikawa, T. 2004. Colourful history of Japan's rat resources. *Nature* 429: 15.
 25. Shisa, H., Lu, L., Katoh, H., Kawarai, A., Tanuma, J., Matsushima, Y., and Hiai, H. 1997. The LEXF: a new set of rat recombinant inbred strains between LE/Stm and F344. *Mamm. Genome* 8: 324–327.
 26. Tokuda, M. 1935. An eighteenth century Japanese guidebook on mouse-breeding. *J. Hered.* 26: 481–484.
 27. Voigt, B., Kuramoto, T., Mashimo, T., Tsurumi, T., Sasaki, Y., Hokao, R., and Serikawa, T. 2008. Evaluation of LEXF/FXLE rat recombinant inbred strains for genetic dissection of complex traits. *Physiol. Genomics* 32: 335–342.
 28. Watanabe, T.K., Suzuki, M., Yamasaki, Y., Okuno, S., Hishigaki, H., Ono, T., Oga, K., Mizoguchi-Miyakita, A., Tsuji, A., Kanemoto, N., Wakitani, S., Takagi, T., Nakamura, Y., and Tanigami, A. 2005. Mutated G-protein-coupled receptor GPR10 is responsible for the hyperphagia/dyslipidaemia/obesity locus of *Dmol* in the OLETF rat. *Clin. Exp. Pharmacol. Physiol.* 32: 355–366.
 29. Yamashita, S., Wakazono, K., Nomoto, T., Tsujino, Y., Kuramoto, T., and Ushijima, T. 2005. Expression quantitative trait loci analysis of 13 genes in the rat prostate. *Genetics* 171: 1231–1238.

¹Department of Nephrology
German Clinic for Diagnostics
Wiesbaden, Germany

²Department of Clinical Social
Medicine, Occupational and
Environmental Dermatology
University Hospital Heidelberg
Heidelberg

E-mail: elke.weisshaar@med.uni-heidelberg.de

Thomas Mettang¹
Uwe Mattered²
Elke Weisshaar²

1. Kittisupamongkol W. Not all that itches is uraemic pruritus. *Nephrol Dial Transplant* 2009; doi: 10.1093/ndt/gfp239
2. Pauli-Magnus C, Mikus G, Alscher DM *et al.* Naltrexone does not relieve uremic pruritus: results of a randomized, double-blind, placebo-controlled crossover study. *J Am Soc Nephrol* 2000; 11: 514–519
3. Neilly J, Martin A, Simpson N *et al.* Pruritus in diabetes mellitus: investigation of prevalence and correlation with diabetes control. *Diabetes Care* 1986; 9: 273–275
4. Weisshaar E, Mattered U, Mettang T. How do nephrologists in haemodialysis units consider the symptom of itch? *Nephrol Dial Transplant* 2009; 24: 1328–1330
5. Zucker I, Yosipovitch G, David M *et al.* Prevalence and characterization of uremic pruritus in patients undergoing hemodialysis: uremic pruritus is still a major problem for patients with end-stage renal disease. *J Am Acad Dermatol* 2003; 49: 842–846
6. Patel TS, Freedman BI, Yosipovitch G. An update on pruritus associated with CKD. *Am J Kidney Dis* 2007; 50: 11–20
7. Ständer S, Weisshaar E, Mettang T *et al.* Clinical classification of itch: a position paper of the International Forum for the Study of Itch. *Acta Derm Venereol* 2007; 87: 291–294

doi: 10.1093/ndt/gfp250

Advance Access publication 27 May 2009

Reduction in urinary excretion of neutrophil gelatinase-associated lipocalin by angiotensin receptor blockers in hypertensive patients

Sir,

We recently read a paper published by Bolignano *et al.* who investigated the association between urinary levels of neutrophil gelatinase-associated lipocalin (Ngal) and severity of renal disease in proteinuric patients [1]. Urinary Ngal is largely and rapidly increased during courses of acute kidney injury (AKI), making it especially useful for early diagnosis of AKI [2–5], but its clinical impact on chronic kidney disease (CKD) remains elusive. They studied non-diabetic patients having >1 g/day of proteinuria at least for 6 months and also healthy subjects, and reported that urinary Ngal concentrations were significantly associated with the extent of proteinuria, and inversely with the estimated glomerular filtration rate. The group also revealed in another study that the elevated urinary Ngal level was a predictor of CKD progression [6].

Our team has also evaluated the correlation between urinary Ngal levels and clinical parameters in CKD patients and observed similar findings. Since the response of urinary Ngal levels to treatment has not been analysed well, here we carried out a prospective observational study. We chose a cohort of 26 hypertensive patients having either

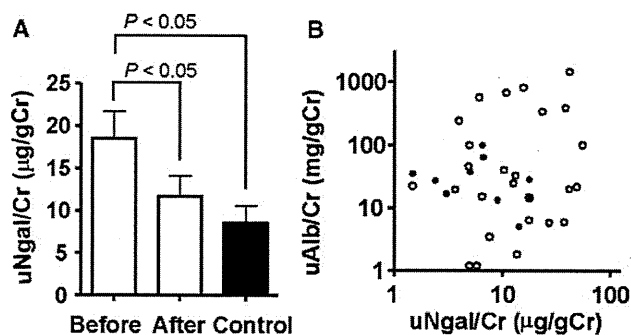


Fig. 1. Urinary Ngal and albumin levels in hypertensive patients having either obesity or diabetes. (A) Mean (\pm SEM) urinary Ngal/urinary creatinine ratios (uNgal/Cr) in patients before and 3 months after treatment with angiotensin receptor blockers, as well as in healthy controls. Comparison was carried out by paired and unpaired *t*-tests. (B) No significant correlation was observed between urinary Ngal and urinary albumin excretion (uAlb/Cr) before the treatment in patients with hypertension (open circles, $n = 26$), when analysed with or without healthy controls (closed circles, $n = 10$), by linear regression analysis.

diabetes ($n = 2$), obesity (15) or both (9), and treated them with angiotensin receptor blockers (ARBs). They included 15 males and 11 females who had ages of 55.5 ± 3.0 years (mean \pm SEM), body mass index of 32.8 ± 1.2 kg/m^2 , serum creatinine of 0.82 ± 0.06 mg/dl and estimated glomerular filtration rate of 79.1 ± 6.5 ml/min/1.73 m^2 (calculated by a Japanese formula revised in year 2009 [7]). Ten healthy volunteers were also studied: 6 males and 4 females with a mean age of 55.7 years. Clinical parameters including urinary Ngal were examined before and 3 months after initiation of the treatment. Hypertension was defined as systolic blood pressure (BP) ≥ 140 , diastolic BP ≥ 90 mmHg or taking antihypertensive reagents. Diabetes was determined as blood HbA1c level $\geq 6.5\%$. Subjects with a body mass index ≥ 25 kg/m^2 were considered obese. Patients neither took any other inhibitors of the renin–angiotensin system, nor were given altered oral regimen during the course. ARBs were chosen from candesartan 12 mg, olmesartan 20 mg or telmisartan 40 mg by the treating physician's preference ($n = 14$, 7 or 5, respectively). The study was carried out in subjects followed at outpatient clinics of Kyoto University Hospital and Kyoto Medical Center, and was approved by ethical committees in those institutes. Patients gave written informed consent.

Before administration of ARBs, hypertensive patients had significantly elevated urinary Ngal levels as compared to healthy controls (Figure 1A). After 3 months of treatment, mean BP was reduced from $158 \pm 3/92 \pm 2$ to $143 \pm 2/82 \pm 2$ mmHg ($n = 26$, $P < 0.001$). All three ARBs similarly decreased systolic and diastolic BP by $\sim 10\%$ (supplementary Table S1). At the same time, urinary excretion of both Ngal and albumin was decreased by 36% (Figure 1A) and 46%, respectively. A similar trend was observed when patients were divided into ones having normoalbuminuria, microalbuminuria or macroalbuminuria ($n = 14$, 6 or 6, respectively; supplementary Table S2). Of note, urinary Ngal and albumin concentrations before ARB treatment were not significantly correlated with each other (Figure 1B, $P > 0.05$), suggesting that these two measurements may

© The Author [2009].

The online version of this article has been published under an open access model. Users are entitled to use, reproduce, disseminate, or display the open access version of this article for non-commercial purposes provided that: the original authorship is properly and fully attributed; the Journal and Oxford University Press are attributed as the original place of publication with the correct citation details given; if an article is subsequently reproduced or disseminated not in its entirety but only in part or as a derivative work this must be clearly indicated. For commercial re-use, please contact journals.permissions@oxfordjournals.org

reflect independent aspects of renal disorders, especially when the level of proteinuria is not very severe.

To our knowledge, this is the first report to show that short-term administration of ARBs significantly reduced urinary Ngal levels in human subjects. Consistently, we have recently observed that ARBs suppressed urinary excretion of Ngal in diabetic mice induced by streptozotocin (STZ) [8]. The concentrations of Ngal were much higher in STZ diabetic mice than human subjects investigated in this study, which may be explained by the difference in the extent of hyperglycaemia and by the species difference concerning Ngal protein metabolism. Furthermore, the treatment of nephrotic patients with steroids and other immune suppressants immediately reduced urinary Ngal excretion [8]. These findings warrant intensive research concerning usefulness of urinary Ngal as a monitoring marker of CKD.

Acknowledgement. This work was in part supported by grant from the Japan Kidney Foundation.

Conflict of interest statement. None declared.

Supplementary data

Supplementary data is available online at <http://ndt.oxfordjournals.org>.

¹Department of Medicine and Clinical Science, Kyoto University
²Clinical Research Institute
³Department of Nephrology, Kyoto Medical Center, Japan
 E-mail: keyem@kuhp.kyoto-u.ac.jp

Masato Kasahara¹
 Kiyoshi Mori¹
 Noriko Satoh²
 Takashige Kuwabara¹
 Hideki Yokoi¹
 Akira Shimatsu²
 Akira Sugawara³
 Masashi Mukoyama¹
 Kazuwa Nakao¹

1. Bolignano D, Coppolino G, Campo S *et al.* Urinary neutrophil gelatinase-associated lipocalin (NGAL) is associated with severity of renal disease in proteinuric patients. *Nephrol Dial Transplant* 2008; 23: 414–416
2. Mori K, Lee HT, Rapoport D *et al.* Endocytic delivery of lipocalin-siderophore-iron complex rescues the kidney from ischemia-reperfusion injury. *J Clin Invest* 2005; 115: 610–621
3. Mishra J, Dent C, Tarabishi R *et al.* Neutrophil gelatinase-associated lipocalin (NGAL) as a biomarker for acute renal injury after cardiac surgery. *Lancet* 2005; 365: 1231–1238
4. Mori K, Nakao K. Neutrophil gelatinase-associated lipocalin as the real-time indicator of active kidney damage. *Kidney Int* 2007; 71: 967–970
5. Coca SG, Yalavarthy R, Concato J *et al.* Biomarkers for the diagnosis and risk stratification of acute kidney injury: a systematic review. *Kidney Int* 2008; 73: 1008–1016
6. Bolignano D, Lacquaniti A, Coppolino G *et al.* Neutrophil gelatinase-associated lipocalin (NGAL) and progression of chronic kidney disease. *Clin J Am Soc Nephrol* 2009; 4: 337–344
7. Matsuo S, Imai E, Horio M *et al.* Revised equations for estimating GFR from serum creatinine in Japan. *Am J Kid Dis*, (2009 Epub)

8. Kuwabara T, Mori K, Mukoyama M *et al.* Urinary neutrophil gelatinase-associated lipocalin levels reflect damage to glomeruli, proximal tubules, and distal nephrons. *Kidney Int* 2009; 75: 285–294

doi: 10.1093/ndt/gfp238

Advance Access publication 27 May 2009

Reply

Sir,

We have read with great interest the results published by Kasahara and co-workers, which confirm that NGAL is becoming more than a promising biomarker of acute renal injury.

Various human studies confirmed the utility of NGAL dosage for the stratification of AKI risk after procedures, potentially detrimental to the kidney. Moreover, it is demonstrated that NGAL plays a role in the onset and progression of chronic kidney disease [1].

Nevertheless, we think that the most interesting NGAL future application could be represented by the evaluation of this marker in response to different acute and chronic therapies. Recently, our group described a strong reduction in urinary NGAL levels in patients affected by steroid-resistant nephrotic syndrome treated with high doses of human immunoglobulins; this reduction was observed immediately after intravenous Ig administration and persisted even 24 h later [2].

If confirmed in different situations, these early variations in NGAL levels could help to predict the effectiveness of different therapeutical approaches, in order to personalize the treatment of nephropathic patients.

Kasahara and co-workers did not describe any relationship between NGAL urinary excretion and albuminuria. Nevertheless, in a recent study conducted on 56 diabetic patients classified according to glomerular damage (normo-, micro- and macroalbuminuria), NGAL levels directly correlated with the severity of the glomerular impairment and they were higher in normoalbuminuric patients than in controls [3]; these findings suggest a parallelism between tubular impairment and glomerular damage and a potential role for NGAL as a marker of diabetic nephropathy even earlier than microalbuminuria.

Enlarging the group of patients affected by arterial hypertension enrolled in the study, we wonder if Kasahara *et al.* may extend their observations also to this pathologic condition, which significantly involves the renal tubule.

Conflict of interest statement. None declared.

Department of Internal Medicine
 University of Messina, Italy
 E-mail: buemim@unime.it

Davide Bolignano
 Michele Buemi

1. Bolignano D, Lacquaniti A, Coppolino G *et al.* Neutrophil gelatinase-associated lipocalin (NGAL) and progression of chronic kidney disease. *Clin J Am Soc Nephrol* 2009; 4: 337–344



Adipose tissue-specific dysregulation of angiotensinogen by oxidative stress in obesity

Sadanori Okada^{a,b,1}, Chisayo Kozuka^{a,1}, Hiroaki Masuzaki^{a,*}, Shintaro Yasue^a, Takako Ishii-Yonemoto^a, Tomohiro Tanaka^a, Yuji Yamamoto^a, Michio Noguchi^a, Toru Kusakabe^a, Tsutomu Tomita^a, Junji Fujikura^a, Ken Ebihara^a, Kiminori Hosoda^a, Hiroshi Sakaue^c, Hiroyuki Kobori^d, Mira Ham^e, Yun Sok Lee^e, Jae Bum Kim^e, Yoshihiko Saito^b, Kazuwa Nakao^a

^aDepartment of Medicine and Clinical Science, Kyoto University Graduate School of Medicine, Kyoto 606-8507, Japan

^bFirst Department of Internal Medicine, Nara Medical University, Kashihara 634-8522, Japan

^cDepartment of Nutrition and Metabolism, Institute of Health Biosciences, The University of Tokushima Graduate School, Tokushima 770-8503, Japan

^dDepartments of Medicine and Physiology, and Hypertension and Renal Center of Excellence, Tulane University Health Sciences Center, New Orleans, LA 70112-2699, USA

^eInstitute of Molecular Biology and Genetics, Seoul National University, Seoul 110-744, South Korea

Received 27 August 2009; accepted 18 November 2009

Abstract

Adipose tissue expresses all components of the renin-angiotensin system including angiotensinogen (AGT). Recent studies have highlighted a potential role of AGT in adipose tissue function and homeostasis. However, some controversies surround the regulatory mechanisms of AGT in obese adipose tissue. In this context, we here demonstrated that the AGT messenger RNA (mRNA) level in human subcutaneous adipose tissue was significantly reduced in obese subjects as compared with nonobese subjects. Adipose tissue AGT mRNA level in obese mice was also lower as compared with their lean littermates; however, the hepatic AGT mRNA level remained unchanged. When 3T3-L1 adipocytes were cultured for a long period, the adipocytes became hypertrophic with a marked increase in the production of reactive oxygen species. Expression and secretion of AGT continued to decrease during the course of adipocyte hypertrophy. Treatment of the 3T3-L1 and primary adipocytes with reactive oxygen species (hydrogen peroxide) or tumor necrosis factor α caused a significant decrease in the expression and secretion of AGT. On the other hand, treatment with the antioxidant *N*-acetyl cysteine suppressed the decrease in the expression and secretion of AGT in the hypertrophied 3T3-L1 adipocytes. Finally, treatment of obese *db/db* mice with *N*-acetyl cysteine augmented the expression of AGT in the adipose tissue, but not in the liver. The present study demonstrates for the first time that oxidative stress dysregulates AGT in obese adipose tissue, providing a novel insight into the adipose tissue-specific interaction between the regulation of AGT and oxidative stress in the pathophysiology of obesity.

© 2010 Elsevier Inc. All rights reserved.

1. Introduction

Overactivity of the systemic renin-angiotensin system (RAS) is one of the central mechanisms for obesity-related

metabolic disorders [1,2]. Notably, the major components of the RAS are expressed in various tissues including the heart, blood vessels, adipose tissue, and brain [3]; these comprise tissue RAS. A series of products are produced locally from

The authors of this manuscript have nothing to declare.

Institutional approval: The human study was approved by the ethics committee for human research of the Kyoto University Graduate School of Medicine (2004, no. 553). Written informed consent was obtained from all subjects prior to the study. All animal experimental procedures were approved by the Kyoto University Graduate School of Medicine Animal Research Committee and the Seoul National University Animal Experiment Ethics Committee.

* Corresponding author. Division of Endocrinology and Metabolism, Second Department of Internal Medicine, Faculty of Medicine, University of the Ryukyus, Okinawa 903-0215, Japan. Tel.: +81 98 895 1145; fax: +81 98 895 1415.

E-mail address: hiroaki@med.u-ryukyu.ac.jp (H. Masuzaki).

¹ Sadanori Okada and Chisayo Kozuka contributed equally to this work.

angiotensinogen (AGT), the unique precursor of angiotensin peptides, and play a critical role in cardiovascular homeostasis [3,4].

Although AGT is produced mainly by the liver, adipose tissue is also considered as a source of AGT production [5]. In agreement with this notion, the adipose tissue expresses all components of the RAS, including AGT, renin, angiotensin I-converting enzyme, and angiotensin II type 1 receptor, in humans and rodents [6,7]. A previous study has demonstrated that AGT-deficient mice are low in blood pressure and body fat mass [8]. Moreover, adipocyte-specific transgenic overexpression of AGT on an AGT-deficient background was shown to augment plasma AGT level and rescue hypotension and leanness [9]. These results indicate that adipose tissue-derived AGT does contribute to the circulating AGT level and adipogenesis.

In rodent experiments, the AGT messenger RNA (mRNA) level in white adipose tissue has been shown to be regulated by the nutritional status; however, that in the liver was independent of the nutritional status [10,11]. In human cross-sectional studies, the AGT mRNA level in adipose tissue was shown to be higher in obese subjects [6,12]. On the other hand, another study reported that the AGT mRNA level in adipose tissue was significantly lower in obese individuals [13]. Elevation of AGT expression in adipose tissue in obese individuals thus remains controversial [14].

Several studies have shown that increased oxidative stress is a manifestation of obesity-related metabolic derangement [15–17]. In fact, in humans, oxidative stress is critically associated with atherosclerosis, hypertension, and diabetes mellitus [18,19]. Oxidative stress is also related with the RAS. Angiotensin II is a potent inducer of reactive oxygen species (ROS) in a variety of tissues [20–22]. In the liver and kidney, increased ROS has been reported to increase AGT gene expression [23–26]. Also in obese adipose tissue, generation of ROS is exaggerated and is involved in adipose tissue dysfunction [17,27]. However, whether increased ROS may affect adipose AGT production remains to be elucidated.

In the present study, we demonstrated that the AGT mRNA level was reduced in obese adipose tissue in humans and mice and in hypertrophied 3T3-L1 adipocytes. In this context, we tested the hypothesis that increased oxidative stress would modulate AGT in obese adipose tissue.

2. Materials and methods

2.1. Subcutaneous abdominal adipose tissue biopsies in human subjects

The present study was performed according to the Declaration of Helsinki and approved by the Ethical Committee on Human Research of Kyoto University Graduate School of Medicine (2004, no. 553). Written informed consent was obtained from all subjects before the study.

Subcutaneous abdominal adipose tissue biopsies were obtained from 46 Japanese subjects (24 men and 22 women; age [mean \pm SD], 46 \pm 2.1 years). The body mass index (BMI) of the subjects ranged from 19 to 52 (mean \pm SD, 30 \pm 1.6) kg/m². All subjects had been on stable therapy with lipid-lowering, antihypertensive, or hypoglycemic agents for at least 1 month before admission and continued with the same doses throughout the study period. Patients who received angiotensin I-converting enzyme inhibitors, angiotensin II receptor blockers, and steroid-related drugs were carefully excluded. For the study, subcutaneous abdominal adipose depots of the study subjects were excised from the periumbilical region under local anesthesia. The samples were immediately frozen in liquid nitrogen and stored at -80°C until use.

2.2. Mouse experiments

Male *ob/ob* mice (age, 12 weeks) were purchased from Oriental BioService (Kyoto, Japan) and housed in the animal facility of Kyoto University. Male *db/db* mice (age, 10 weeks) were purchased from Japan SLC (Hamamatsu, Japan) and housed in Seoul National University. The mice were allowed free access to food and water. For in vivo antioxidant treatment, the *db/db* mice were injected with *N*-acetyl cysteine (NAC; 150 mg/kg body weight; Sigma-Aldrich Japan, Tokyo, Japan) or the vehicle (phosphate-buffered saline) into the peritoneal cavity once daily for 1 week. All experimental procedures were approved by the Kyoto University Graduate School of Medicine Animal Research Committee and the Seoul National University Animal Experiment Ethics Committee.

2.3. Cell culture and isolation of primary adipocytes

3T3-L1 fibroblasts were cultured and differentiated into adipocytes as described previously [28]. Briefly, the 2-day postconfluent cells (designated as day 0) were incubated for 2 days with 10% fetal bovine serum (FBS)/Dulbecco modified Eagle medium (DMEM), 0.5 mmol/L 3-isobutyl-1-methylxanthine, 0.25 $\mu\text{mol/L}$ dexamethasone, and 1 $\mu\text{g/mL}$ insulin. The cells were then incubated for 2 days in 10% FBS/DMEM with insulin and, thereafter, incubated in 10% FBS/DMEM that was changed on every alternate day. Oil red O staining was performed as described [29].

Primary adipocytes were isolated from epididymal fat pads of 9-week-old male C57BL/6J mice (purchased from Oriental BioService, Kyoto, Japan). Epididymal fat pads were harvested, minced into 2- to 3-mm pieces, and digested using 0.8 mg/mL collagenase (Sigma-Aldrich Japan) in DMEM for 30 minutes at 37°C in a shaking water bath. After the digestion with collagenase, cells were filtered through a 250- μm nylon filter and centrifuged at 1000 rpm for 30 seconds. The suspended mature adipocytes were separated from the pelleted stromovascular fraction and washed 3 times in DMEM for experiments.

2.4. Determination of adipocyte size

The cells were fixed with 2% osmium tetroxide and passed through a 250- μ m nylon filter to remove the fibrous elements, and the cells were washed extensively with isotonic saline. A total of 10 000 cells was analyzed using the Coulter Multisizer III (Beckman Coulter, High Wycombe, England) [30].

2.5. Quantitative real-time polymerase chain reaction

Total RNA was extracted from human and mouse adipose tissue by using a QIAGEN RNeasy Mini Kit (QIAGEN Japan, Tokyo, Japan) and from cultured adipocytes by using Trizol Reagent (Invitrogen, Carlsbad, CA). Complementary DNA was then synthesized by using an iScript cDNA Synthesis Kit (Bio-Rad, Hercules, CA). Taqman polymerase chain reactions (PCRs) for human AGT, mouse AGT, mouse monocyte chemoattractant protein 1 (MCP-1), mouse interleukin 6 (IL-6), and mouse tumor necrosis factor α (TNF α) were performed using the ABI Prism 7300 Sequence Detection System (Applied Biosystems, Foster City, CA). The sequences of probes and primers are summarized in Table 1.

2.6. Enzyme-linked immunosorbent assay

The AGT protein level in the culture media was measured by sandwich-type enzyme-linked immunosorbent assay (ELISA) as described [31]. Similarly, the MCP-1 and IL-6 protein levels were detected by using an ELISA kit (R&D Systems, Minneapolis, MN).

2.7. Determination of ROS

The ROS activity was determined by the nitroblue tetrazolium (NBT) assay [32]. Reduced NBT (formazan) was dissolved in 50% acetic acid, and the absorbance of the supernatant was determined at 560 nm.

2.8. Statistical analysis

The data are presented as the mean \pm SE. Unpaired Student *t* test was used for comparisons with the control

group. The differences were accepted as significant at a level of $P < .05$.

3. Results

3.1. AGT mRNA expression level in adipose tissue from obese humans and mice

To explore the impact of obesity on AGT gene expression in human adipose tissue, we performed subcutaneous abdominal adipose tissue biopsies from 46 subjects with a wide range of BMI. The AGT mRNA level was significantly reduced by 61% in the obese subjects as compared with the nonobese subjects (Fig. 1A).

To verify the obesity-related decrease in adipose AGT expression, we analyzed adipose tissue from genetically obese mice. In 12-week-old male *ob/ob* mice (mean body weight, 60 \pm 0.7 g), the AGT mRNA level was significantly decreased in both epididymal (29%) and subcutaneous (57%) adipose depots as compared with their lean littermates (mean body weight, 29 \pm 0.3 g) (Fig. 1B). On the other hand, the AGT mRNA levels in the liver remained unaltered in both groups (Fig. 1C).

Similar results were observed in case of the diet-induced obese (DIO) mice (12-week-old male C57BL/6J mice fed with a high-fat/high-sucrose diet for 4 weeks). The AGT mRNA level in the adipose tissue of the DIO mice (mean body weight, 40 \pm 0.8 g) was significantly lower than that in the adipose tissue of their lean littermates (mean body weight, 30 \pm 0.4 g) ($P < .05$); however, the hepatic AGT mRNA level remained unchanged in both groups (Yasue et al, unpublished observations). These results indicate that the AGT mRNA level was decreased exclusively in the obese adipose tissue in both humans and mice.

3.2. AGT expression during the course of hypertrophy in the 3T3-L1 adipocytes

To explore the mechanism by which AGT is decreased in obese adipose tissue, we analyzed hypertrophied adipocytes. 3T3-L1 fibroblasts were completely differentiated into

Table 1
Sequences of Taqman PCR primers and probes

Gene name Genbank accession no.	Forward primer Reverse primer	Probe (5'-FAM, 3'-TAMRA)
Human AGT NM_000029	GGTGGAGGGTCTCACTTTCCA ATGGTCAGGTGGATGGTCCG	CCCTCAACTGGATGAAGAACTGTCTCC
Mouse Agt NM_007428	ACACCTACGTTCACTTCCAAG CCGAGATGCTGTTGTCCAC	ATGAGAGGTTTCTCTCAGTGCCTGGA
Mouse Ccl2 (MCP-1) NM_011333	TTGGCTCAGCCAGATGC CCAGCCTACTCATTGGGATCA	CCCCACTCACCTGCTGCTACTCATTCA
Mouse Il6 (IL-6) NM_031168	ATGAAGTTCCTCTCTGCAAGAG GTAGGGAAGGCCGTGGTTG	CACCAGCATCAGTCCCAAGAAGGCA
Mouse Tnf (TNF α) NM_013693	TCTCTCAAGGGACAAGGCTG ATAGCAAATCGCTGACGGT	CCCGACTACGTGCTCCTCACCCA

The sequences of primers and probes for each gene used in the present study are summarized.

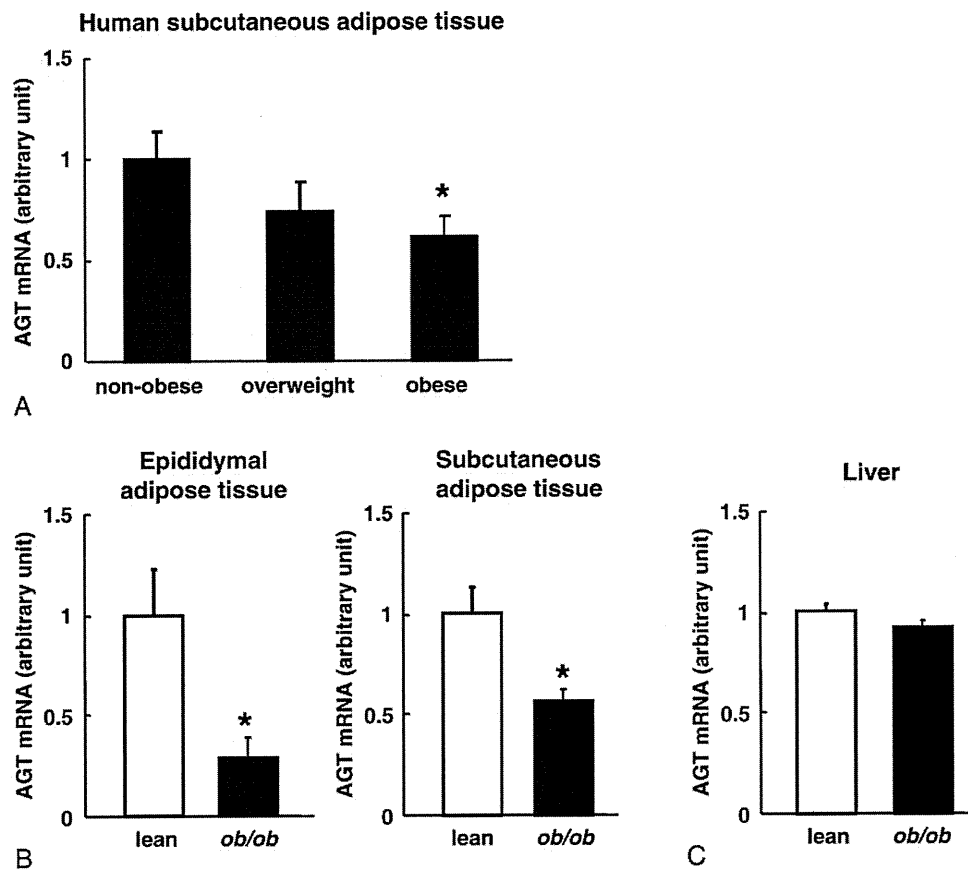


Fig. 1. The AGT mRNA levels in obese adipose tissue from humans and mice. A, The relation between the AGT mRNA level in subcutaneous abdominal adipose tissue and the degree of obesity in humans: nonobese (BMI <25), n = 20; overweight (25 ≤ BMI <30), n = 13; obese (BMI ≥30), n = 13. B, Comparison of the adipose tissue AGT mRNA levels in 12-week-old male *ob/ob* mice (n = 4; mean body weight, 60 ± 0.7 g) and their lean littermates (n = 4; mean body weight, 29 ± 0.3 g). Left: epididymal adipose tissue depots. Right: subcutaneous abdominal adipose tissue depots. C, Comparison of the hepatic AGT mRNA level between the *ob/ob* mice (n = 4) and their lean littermates (n = 4). The mRNA level was examined by real-time PCR and normalized to that of 18S ribosomal RNA (rRNA). The data are expressed as the mean ± SE. *P < .05 as compared with the nonobese subjects or the lean littermates.

adipocytes for 8-day incubation with induction media [28]. Consistent with a previous report [33], the AGT mRNA level in differentiated 3T3-L1 adipocytes (day 8) was significantly elevated by 15-folds in comparison with 3T3-L1 fibroblasts (day 0). For generating hypertrophied adipocytes, 3T3-L1 adipocytes were cultured up to 30 days after the induction of differentiation. Oil red O staining exhibited a gradual increase in lipid accumulation from day 8 to day 28. The adipocytes displayed unilocular lipid droplets on days 18 and 28 (Fig. 2A).

The mean diameter of the adipocytes as assessed by the Coulter Multisizer III was 20.2 μm on day 8 and 37.5 μm on day 30 (Fig. 2B). During the course of adipocyte hypertrophy, ROS production increased 2.7-folds (day 18) and 4.3-folds (day 28) in comparison with the levels on day 8 (Fig. 2C). The mRNA and protein levels of MCP-1 and IL-6 were elevated substantially on days 18 and 28 (Fig. 2D and E, respectively). The AGT mRNA level was significantly lower on days 18 (48%) and 28 (42%) than that on day 8 (Fig. 2D). The AGT concentration in the culture media was decreased on days 18 (59% of the initial value) and 28 (42%

of the initial value) (Fig. 2E). These results suggest that AGT expression and secretion were decreased in the hypertrophied adipocytes.

3.3. Impact of TNFα on the expression and secretion of AGT in adipocytes

Tumor necrosis factor α plays a critical role in the pathophysiology of inflammation and oxidative stress [27,34,35]. To explore the impact of TNFα on the expression and secretion of AGT in adipocytes, the differentiated 3T3-L1 adipocytes (day 8) were treated with TNFα (Sigma-Aldrich Japan) for 24 hours. Treatment with TNFα decreased the AGT mRNA level in a dose-dependent manner along with a concomitant increase in the MCP-1 and IL-6 mRNA levels (Fig. 3A). The AGT protein level in the culture media decreased in parallel to the AGT mRNA level (Fig. 3B).

We also investigated the effects of TNFα on primary adipocytes. Similarly to 3T3-L1 adipocytes, treatment with TNFα (10 ng/mL) for 24 hours slightly but significantly decreased AGT mRNA level and substantially increased MCP-1 mRNA level (Fig. 3C).

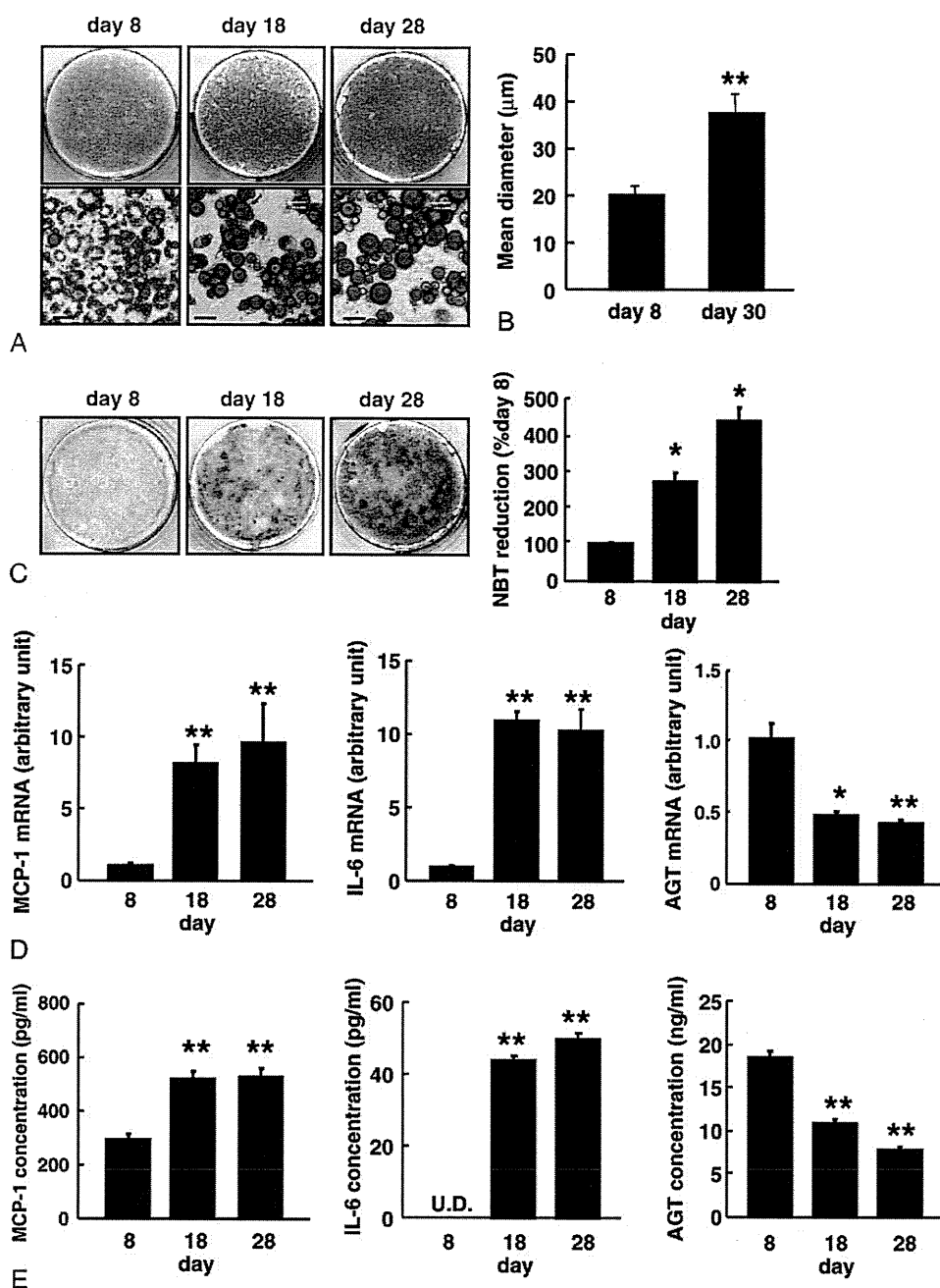


Fig. 2. The AGT expression during the course of hypertrophy in the 3T3-L1 adipocytes. A, Oil red O staining of the 3T3-L1 adipocytes on days 8, 18, and 28 after induction of differentiation. Bar = 30 μm . B, Size of the 3T3-L1 adipocytes on days 8 and 30. Adipocyte size was measured using a Coulter Multisizer III. C, The ROS production during adipocyte hypertrophy. The ROS production was assessed by the NBT assay. Dark blue formazan was dissolved, and the absorbance was determined at 560 nm ($n = 3$). D, The MCP-1, IL-6, and AGT mRNA levels in the 3T3-L1 adipocytes on days 8, 18, and 28 ($n = 4$). The mRNA level was examined by real-time PCR and normalized to that of 18S rRNA. E, The AGT protein concentration in the culture media. The MCP-1, IL-6, and AGT concentrations in the 3T3-L1 adipocytes on days 8, 18, and 28 were analyzed by ELISA ($n = 4$). Results are representatives of at least 3 independent experiments. The data are expressed as the mean \pm SE. * $P < .05$ and ** $P < .01$ as compared with the value of day 8. U.D. indicates undetectable.

3.4. Impact of oxidative stress on the expression and secretion of AGT in adipocytes

To explore the impact of oxidative stress on the expression and secretion of AGT in adipocytes, differentiated 3T3-L1 adipocytes (day 8) were exposed to a specific

ROS molecule, hydrogen peroxide (H_2O_2), for 24 hours [17,36]. Incubation of adipocytes with H_2O_2 significantly increased the MCP-1 mRNA level, consistent with a previous report [17]. In contrast, H_2O_2 diminished the AGT mRNA level up to 35% of the initial value in a dose-dependent manner (Fig. 4A). The AGT protein level in the

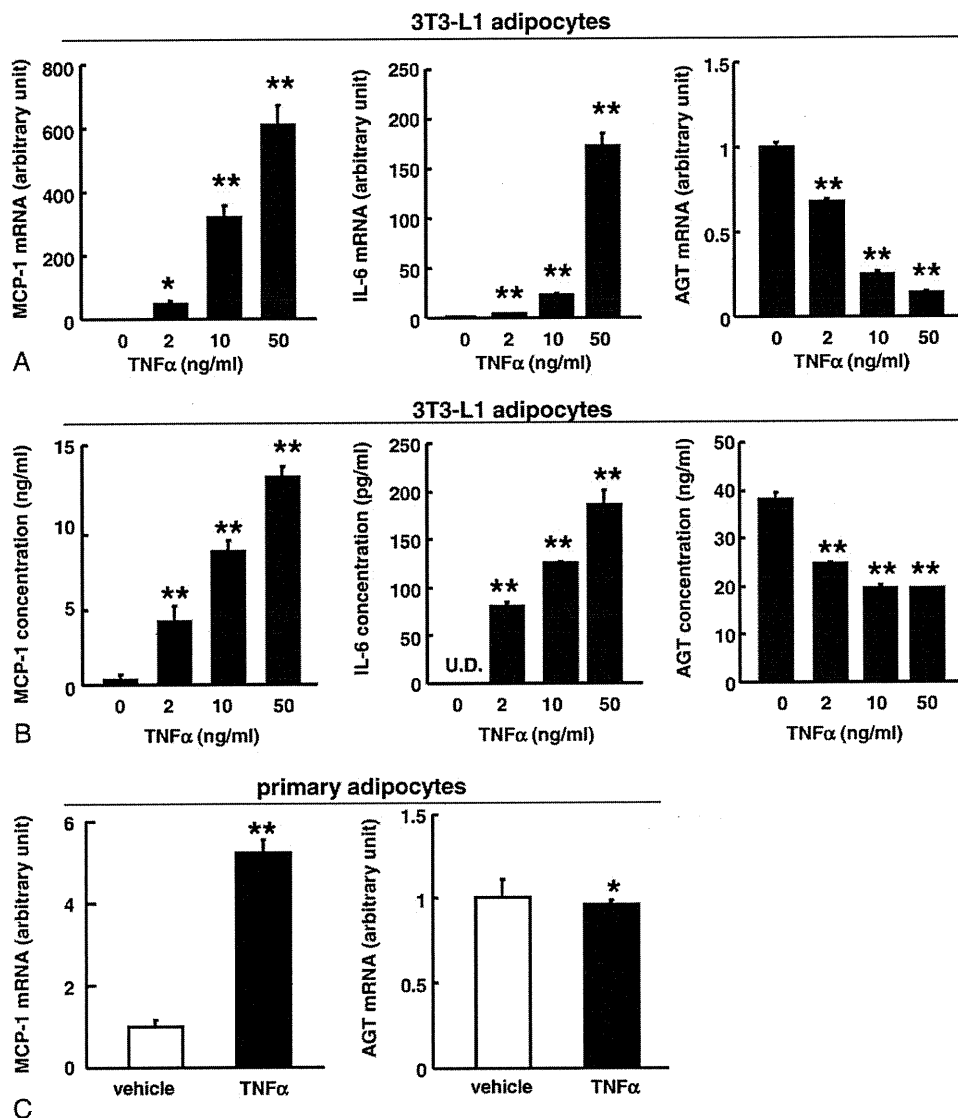


Fig. 3. Impact of TNF α on the expression and secretion of AGT in the 3T3-L1 adipocytes. A, The AGT, MCP-1, and IL-6 mRNA level in the 3T3-L1 adipocytes (day 8) treated with TNF α for 24 hours (n = 4). The mRNA level was examined by real-time PCR and normalized to that of 18S rRNA. B, The AGT protein concentration in the culture media in the 3T3-L1 adipocytes (day 8) treated with TNF α for 24 hours (n = 4). The protein level was assessed by ELISA. C, The AGT and MCP-1 mRNA level in the primary adipocytes treated with TNF α (10 ng/mL) for 24 hours (n = 4). The mRNA level was examined by real-time PCR and normalized to that of 18S rRNA. Results are representatives of at least 3 independent experiments. The data are expressed as the mean \pm SE. * P < .05 and ** P < .01 as compared with the control value.

culture media also decreased up to 23% of the initial value (Fig. 4B).

Similar to 3T3-L1 adipocytes, H₂O₂ treatment (1 mmol/L, 24 hours) significantly decreased AGT mRNA level in primary adipocytes (Fig. 4C). The H₂O₂ treatment tended to increase the MCP-1 mRNA level.

3.5. Effect of antioxidant treatment on the expression and secretion of AGT in adipocytes

We examined whether inhibition of ROS generation could nullify the decrease in AGT gene expression and AGT secretion in obese adipose tissue. First, we treated 3T3-L1 adipocytes with the antioxidant NAC (10 mmol/L) for 10

days (days 8–18). Without the NAC treatment, the adipocytes had become hypertrophic and increased ROS production in this period (Fig. 2B and C). The NBT assay revealed that NAC treatment significantly suppressed ROS production (Fig. 5A). Although ROS production was reported to potentiate adipocyte differentiation in early phase [37], the ROS suppression with the NAC treatment in our experiments did not cause morphologic changes in hypertrophied adipocytes compared with the vehicle treatment. The NAC treatment inhibited the increase in MCP-1 expression (Fig. 5B). The AGT mRNA level was significantly elevated with NAC treatment (Fig. 5B).

To test whether such phenomenon is reproducible in obese adipose tissue where ROS production is exaggerated

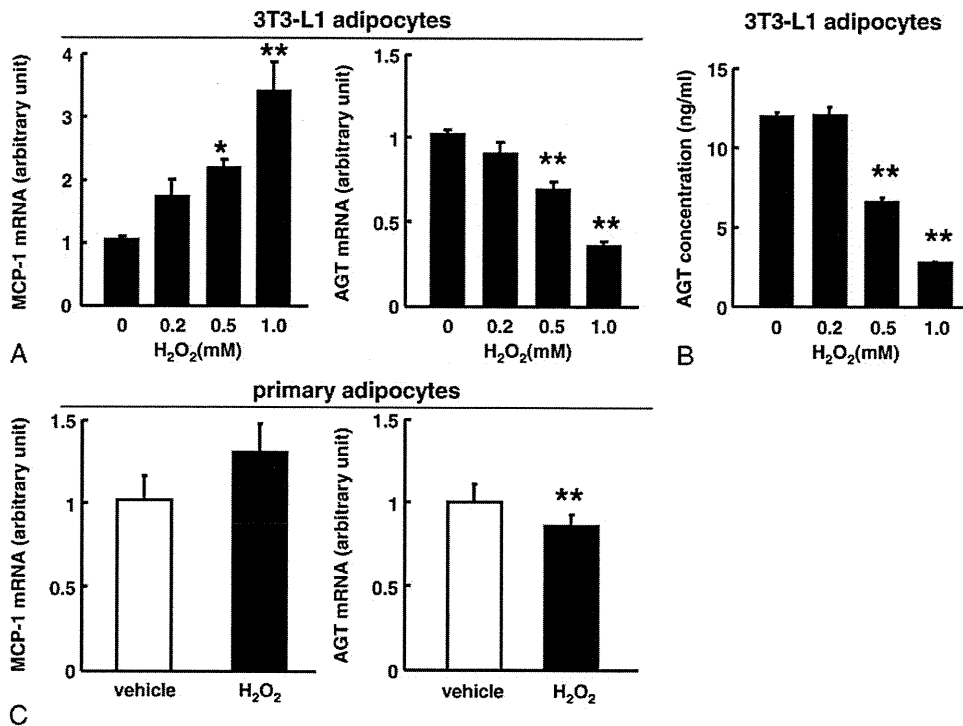


Fig. 4. Impact of oxidative stress on the expression and secretion of AGT in the 3T3-L1 adipocytes. A, The AGT and MCP-1 mRNA level in the 3T3-L1 adipocytes (day 8) treated with H₂O₂ for 24 hours (n = 4). The mRNA level was examined by real-time PCR and normalized to that of 18S rRNA. B, The AGT protein level in the culture media of the 3T3-L1 adipocytes (day 8) treated with H₂O₂ for 24 hours (n = 4). The protein concentration was assessed by ELISA. C, The AGT and MCP-1 mRNA level in the primary adipocytes treated with H₂O₂ (1 mmol/L) for 24 hours (n = 4). The mRNA level was examined by real-time PCR and normalized to that of 18S rRNA. Results are representatives of at least 3 independent experiments. The data are expressed as the mean ± SE. *P < .05 and **P < .01 as compared with the control value.

[17], we administered NAC to obese *db/db* mice once daily for 1 week. Similar to the obese *ob/ob* mice and DIO mice, in obese *db/db* mice (mean body weight, 48 ± 1.5 g), the AGT mRNA level in epididymal adipose tissue was markedly decreased to 22% as compared with their lean littermates (mean body weight, 28 ± 1.0 g) (Fig. 5C). In contrast, the TNF α mRNA level in epididymal adipose tissue was significantly higher in *db/db* mice than in their lean littermates (Fig. 5C). Both systemic and local (adipose tissue) oxidative stress was elevated substantially in obese *db/db* mice [38]. Notably, in *db/db* mice, NAC treatment significantly reduced the oxidative stress also in adipose tissue [38].

In the NAC treatment group, the AGT mRNA level in the epididymal adipose depots increased significantly by 2.1-folds compared with that in the vehicle group, whereas the IL-6 ($P = .052$) and TNF α ($P = .10$) mRNA levels tended to decrease in the NAC treatment group (Fig. 5D). On the other hand, the hepatic AGT mRNA level remained unchanged in both groups (Fig. 5E).

4. Discussion

The major finding of the present study is that oxidative stress dysregulates AGT in adipose tissue in obese humans

and rodents. The AGT mRNA level was decreased in both obese adipose tissue and hypertrophied adipocytes, in which oxidative stress was exaggerated. Exposure of oxidative stress decreased AGT expression not only in the adipocyte cell line but also in primary adipocytes. The decrease in AGT expression was rescued by treatment with the antioxidant both in vivo and in vitro. Such obesity-associated changes in AGT in the adipose tissue were not observed in the liver.

The AGT regulation in obese adipose tissue has long been analyzed, but results were inconsistent [6,12,13]. We here demonstrated that the AGT mRNA level in adipose tissue was reduced in both obese humans and mice (Fig. 1). In obese mice, there seem to be no apparent depot-specific (subcutaneous and epididymal adipose depots) or strain-specific (*ob/ob*, *db/db*, and DIO mice) differences in the fall of AGT in adipose tissue. The AGT mRNA level was decreased also in hypertrophied 3T3-L1 adipocytes (Fig. 2). These results are consistent with a previous report using differentiation system of human adipocytes in primary culture, where the AGT mRNA level increased in differentiation process, but decreased in further culture process [39].

In previous experiments, several hormonal and metabolic changes associated with obesity influence AGT expression in adipocytes; however, due to species differences and experimental conditions, there are controversies around the results [39–42]. On the other hand, our results indicate that